Used Lithium-Ion Batteries in Second-Life Applications: Feasibility Study

Minh Tran
Department of Electrical Engineering
Tampere University
Tampere, Finland
minh.tran@tuni.fi

Tuomas Messo
Department of Electrical Engineering
Tampere University
Tampere, Finland
tuomas.messo@tuni.fi

Roni Luhtala
Department of Electrical Engineering
Tampere University
Tampere, Finland
roni.luhtala@tuni.fi

Jussi Sihvo
Department of Electrical Engineering
Tampere University
Tampere, Finland
jussi.sihvo@tuni.fi

Tomi Roinila
Department of Electrical Engineering
Tampere University
Tampere, Finland
tomi.roinila@tuni.fi

***Abstract*—Lithium-ion (Li-ion) batteries have become key factors in powering various consumer products and industrial loads. However, the increase in battery production has raised environmental issues as approximately 95 percent of Li-ion batteries are landfilled upon reaching end of life. Studies suggest, however, that almost 95 percent of Li-ion batteries could be recycled, for example, in second-life applications. A conventional method to characterize a battery is to use the battery state-of-charge (SOC) and state-of-health (SOH). These quantities can be used for predicting the remaining battery life cycle and for selecting reusable batteries. However, measuring the SOC and SOH is difficult using existing technology. Recent studies have shown that the SOC and SOH can be evaluated using the battery internal impedance. This paper demonstrates the applicability of the internal impedance in evaluating the suitability of used Li-ion batteries in second-life applications. Experimental measurements are shown from several commercial Li-ion batteries.**

***Index Terms*—batteries, energy storage, impedance measurement, second-life applications**

I. Introduction

The number of applications involving Li-ion batteries has rapidly increased in recent years. The global Li-ion battery market size is projected to reach approximately 100 billion euros by 2030. However, this number only applies mainly to the technology based on automotive and renewable energy production. For example, mining equipment industry is expected to reach 115 billion euros in 2025, and half of the equipment sold in 2025 will have on-board Li-ion battery packs [1].

Approximately 95 percent of all Li-ion batteries (1M tons' worth per year) are landfilled instead of recycled upon reaching end of life. The main reason is behind the fact that most industrialized recycling processes are limited and only capable of recovering raw materials. Li-ion batteries in landfills may catch fire or, if the electrolyte is exposed to water, hydrogen fluoride formation can occur. All of these are non-options for a sustainable future. However, studies suggest that almost 95 percent of the battery waste could be recycled [2]. This number includes the material recycling as well as the battery recovery for second-life applications. The latter one applies particularly on Li-ion batteries used in electric vehicle applications in which the battery is considered no longer suitable for the vehicle when it degrades less than 80 percent of its original capacity [3]. It is estimated that second-life battery capacity produced by electric vehicles will soon hit over 275 GWh per year which presents huge opportunities for different energy storages [4]–[6]. One option would be using this capacity in grid-level storage devices. There are sophisticated technologies to extract and recycle usable minerals from used cells, but there currently exists no feasible method to determine cells that are still usable.

Li-ion batteries can be dynamically characterized by using the battery state-of-charge (SOC) and state-of-health (SOH) [7], [8]. However, obtaining these quantities directly is difficult. For example, the battery capacity, which is required for the SOH estimation, is challenging to measure when the battery is operating due to relatively long measurement time. Usually, the capacity must be estimated using the voltage, current and temperature measurements after which an aging model is applied [9].

Studies have shown that the battery SOH strongly depends on the battery internal impedance [7]. The impedance is shown to be affected by the battery aging mechanisms at different frequencies, and therefore, the impedance provides a highly potential method to analyze the battery capacity and power capability. As the impedance can be measured without breaking the battery, the method can be conveniently performed in real time.

This paper demonstrates how the battery internal impedance can be used to provide predictive information about the battery viability for second-life applications. Several experimental measurements are shown by using used commercial Li-ion batteries. The main goal is to provide a method which can be utilized for a battery SOH estimation based on impedance measurement. The results can be applied both in on-board

applications where the battery is analyzed in real time or in analysis of used batteries in defining their capability to operate in a second-life application.

The remainder of the paper is organized as follows. Section II provides theoretical basis for the ageing mechanisms of the battery and how they are related to the lifecycle. Section III presents the methods for battery impedance measurement. Section IV presents experimental measurements based on several commercial Li-ion battery cells. Finally, Section V draws conclusions.

II. Theory

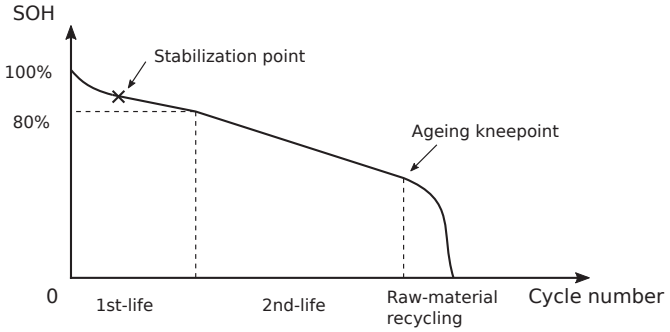

Fig. 1: SOH curve of a Li-ion cell life cycle.

Fig. 1 demonstrates a conceptual life cycle of a Li-ion battery cell in terms of cycle number and SOH, typically expressed as a percentage of the current maximum storage capacity out of the rated capacity [10]. The life cycle can be divided into three parts: first-life application, second-life application and the final raw-material extraction at the recycling factory. First-life applications typically include electric vehicles and consumer electronics. First life spans from the first cycle until the capacity loss reaches more than the typical 20% limit. After that, the cell is disposed of for recycling or switched to second-life use. Second-life applications can be, for example, energy storages for grid-connected photovoltaic power systems. Once the SOH reaches the ageing kneepoint, upon which the positive feedback of degradation causes a rapid drop in charge capacity, the cell is considered unusable [11], [12]. Second-life viability of a Li-ion battery cell can then be characterized by the amount of charge the cell can supply before reaching the ageing kneepoint.

Li-ion battery degradation is characterized by the loss of energy storage capacity and power capability over time. The degradation is typically described by measurable variables such as charge-capacity fading and increase of the battery cell internal resistance [10], [13], [14]. Loss of capacity and increased internal resistance are caused by various naturally-occured ageing processes such as corrosions of electrode materials, increasing thickness of the solid-electrolyte interface (SEI) layer and lithium plating. External factors such as high load current, high temperature, overvoltage and overdischarge accelerate the speed of the ageing processes and consequently lead to shorter lifetime.

The most dominant ageing mechanism in a Li-ion battery cell is the growth of the solid-electrolyte interface (SEI) layer that exists between carbonaceous negative-electrode materials such as graphite and the electrolyte solution inside the cell. As the cell charges and discharges many cycles over time, the thickness and coverage of the SEI layer increase by consuming both the negative electrode and the electrolyte material. The SEI layer, although serves as a stabilizing substance for the cell, consumes the lithium ions inventory as it grows, resulting in more loss of charge capacity of the cell. Increased SEI thickness also results in higher inhibition of ionic flow, hence higher internal resistance overtime. Increased internal resistance leads to decreased efficiency, lower power output limit and decreased safety margin.

The main degradation mechanism at the end of the usuable lifetime of a Li-ion battery is the formation of lithium dendrite, or lithium plating. Lithium dendrites are formed on the surface of the SEI layers due to the uneven distribution of ionic flow and ionic concentration in the electrolyte and in the electrodes. The lithium plating process is magnified at high charge/discharge current or high temperature. When the dendrite is long enough, it reaches through the separator and short-circuits the two electrodes with electronic flow. The short circuit results in thermal runaway, which is highly dangerous as the fire is self-sustainable.

As Fig. 1 demonstrates, the cell SOH experiences an initial rapid drop in the beginning due to the increasing consumption of lithium ions by the SEI layer inside the cell structure [13]. The speed of capacity fading then reduces as the SEI layer thickens and stabilizes. SEI stabilization inhibits further decomposition of electrode materials, resulting in a fairly linear drop of capacity as the cycle number progresses. As the lifecycle continues, the SOH reaches the ageing kneepoint where the maximum charge capacity suffers a sudden rapid drop. At this point, the rate of capacity fading changes from linear to nonlinear. The ageing knee is typically associated with excessive formation of lithium dendrite beyond a stable limit [15]. Identification of the ageing knee based on internal resistance gives a termination condition for second-life operations of a Li-ion battery cell.

III. Methods

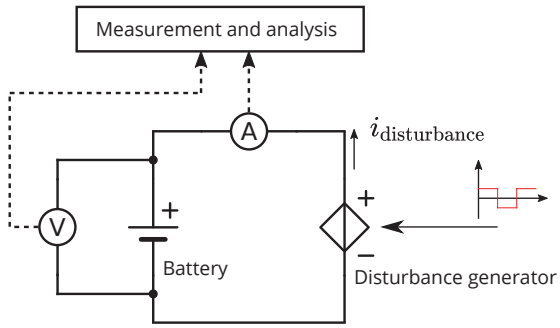

Fig. 2: Conceptual battery internal impedance measurement setup.

Studies have shown the use of the battery cell internal impedance as a convenient SOH indicator [16]–[20]. The internal impedance provides direct information of the dynamic processes inside a battery cell which gives useful information about the battery states. The impedance can be easily found by measuring the cell current and voltage signals. The basic principle for measuring the battery cell internal impedance is demonstrated in Fig. 2. An external current disturbance is applied to charge and discharge the battery. This produces a voltage response at the battery terminals. The resulting current and output voltage are measured, and Fourier transform is applied to obtain the spectral information of the impedance.

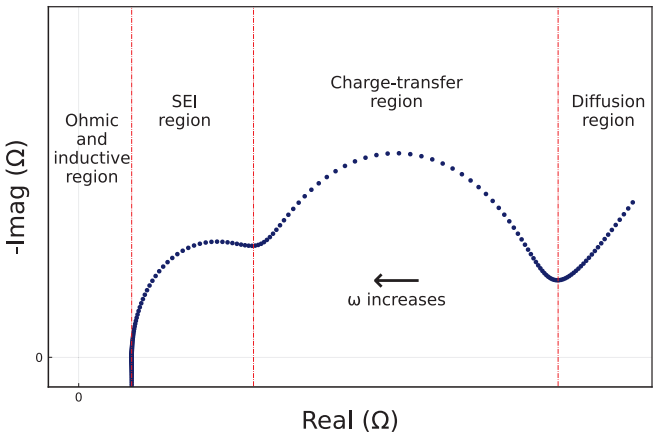

Fig. 3: Nyquist plot of a Li-ion battery impedance.

Fig. 3 shows a typical impedance spectra of a Li-ion battery as a Nyquist plot. The imaginary axis is most often inverted so that the capacitive characteristic of the impedance is shown in the first quadrant of the complex plane. The curve can be divided into different regions that signify different electrochemical processes in the battery. At low frequencies, typically less than a few hundreds mHz, diffusion processes dominate the electrodes and are represented by a $45°$ rising line in the Nyquist plot. In the mid-frequency region, ranging between several mHz to a few KHz, semicircular arches representing the charge-transfer (CT) region and the SEI region characterize the movement of ions between the electrodes, the SEI layers and the electrolyte. At higher frequencies, the impedance values enter the ohmic and inductive region where the inductive behavior describes the overall dynamics for the conduction parts of the battery.

The battery internal impedance is conventionally obtained by applying electrochemical spectroscopy (EIS) [21]. In the method, the battery is perturbed by sinusoidal waves at various frequencies. The conventional EIS, however, is difficult to implement in practical applications due to many signal levels and long measurement time. Another method to estimate the battery internal impedance is by applying hybrid pulse power characterization (HPPC) current test profile to collect the time-domain voltage response, the values of which can be used to deduce internal resistance and equivalent capacitance value of the cell [22]. The method is simple in practice but can be inaccurate and cannot be used at extreme cell SOC conditions due to high disturbance current amplitude.

Recent studies have presented impedance-measurement methods based on broadband perturbations [23]–[26]. In the methods the battery under test is perturbed by periodic binary signals such as the pseudorandom binary sequence (PRBS). Measuring the impedance using the PRBS significantly shortens the measurement time compared to the traditional EIS as the signal carries energy at several frequencies in a single injection period. In addition, as the PRBS is in binary form, the signal can be generated using low-cost signal generators the output of which can only cope with a small number of signal levels [27].

IV. Experiments

Several experimental measurements were carried out to demonstrate the effectiveness of the battery internal impedance in defining the battery SOH. The batteries under test were obtained from a recycling plant making them ready for second-life application testing. The cells have 2050 mAh nominal charge-capacity and 1.075 A standard charge current.

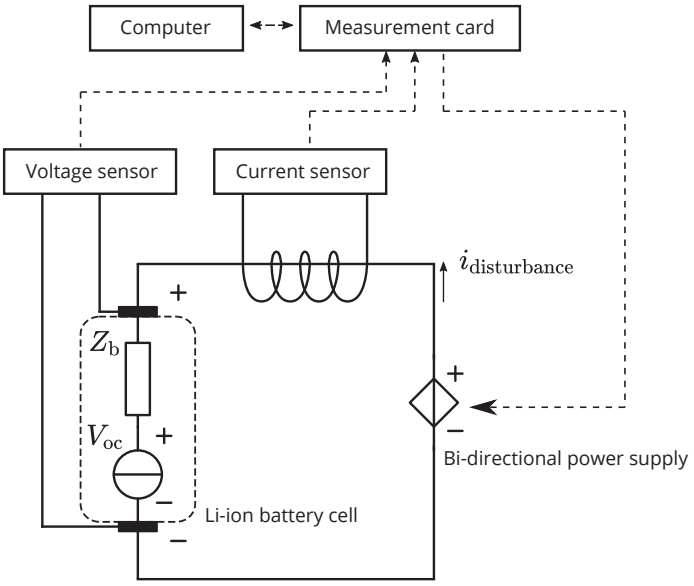

Fig. 4: Impedance measurement setup

The internal impedance of each cell was measured in the beginning of the experiment. Fig. 4 demonstrates the experimental setup used to obtain the battery cell impedance. As the experiment starts, an excitation voltage signal is generated by the measurement card (NiDAQ USB-6363). The generated signal is transformed into current injection ($i_{\text{disturbance}}$) by the bi-directional power supply (KEPCO BOP 50-20MG) acting as a controlled current source. In order to obtain rapid impedance measurement, PRBS excitation was used. The PRBS amplitude was selected as 0.5 amperes and the generation frequency was selected as 6 kHz. The injection was done in two separate injections. The first injection covered the measurement bandwidth from 1 mHz to 10 Hz and the

second injection from 10 Hz to 2 kHz. The cell voltage and input current were measured by a voltage sensor (coaxial cable connected directly to the cell terminals) and a current sensor (Tektronix TCPA300). The measured signals were collected by the measurement card at 480 kHz sampling rate. Finally, the measurement card sent the collected signals to the computer for signal processing. The Fourier transform was applied to the measured voltage and current to obtain the spectral data of the internal impedance.

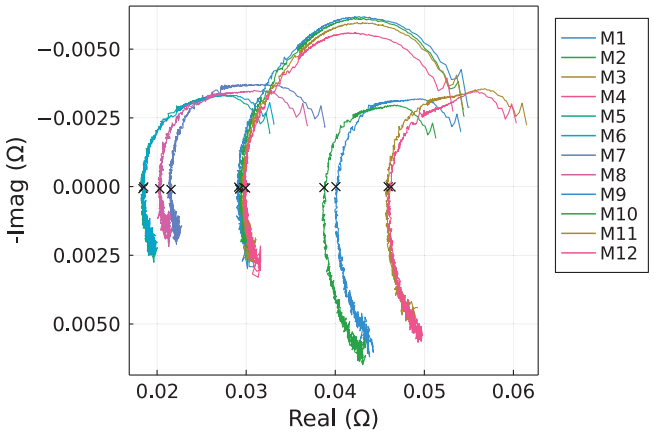

Fig. 5: Impedance measurements

Fig. 5 shows the measured impedance curves of the cells shown in a Nyquist plot. The cell internal resistance, typically found around 1 kHz, is marked as black crosses on the real axis. Ageing acceleration process then starts for all the cells at standard charge/discharge current level (0.5C) and at room temperature (25°C). One charge/discharge cycle is equivalent to fully discharging a cell from 100% SOC to 0% SOC, and then charging the cell back to 100% SOC. Maximum charge-capacity value was recorded for each cell at every cycle. The cells were cycled up to 800 cycles.

Figs. 6a - 6b show the maximum charge-capacities for each cell as a function of cycle number. Cells M1 to M4 have shorter cycling due to rapid loss of capacity during the cycling. Otherwise, the capacity values of the other cells remain above 70 percent of the initial value up to 500 cycles. Some of the cells start to reach the ageing kneepoint as reflected by a more rapid loss of capacity as early as 500 cycles, while the other cells showed relatively linear capacity fading, indicating longer usable life.

Fig. 5 clearly shows the relation between the impedances and capacity values of the cells shown in Figs. 6a - 6b. For example, cells M3 and M4 lose their capacity faster than any other cell. At the same time their impedances have the largest real parts, that is, they are located more on the right side of the complex plane. Cells M1 and M2 have slightly smaller real parts and they also lose capacity slower than M3 and M4. Cells M5 to M8 on the other hand have the smallest real parts and their capacity remains higher compared to other cells. The impedances of cells M9 to M12 are located in between on the

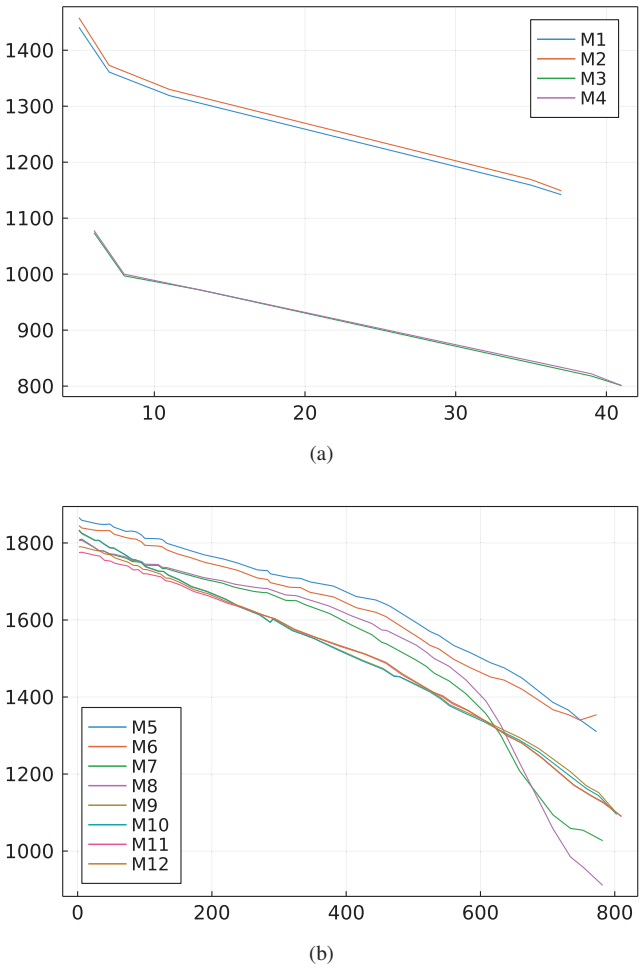

Fig. 6: Capacity drops of a) poor cells and b) other cells.

complex plane and their capacity fade is also in between the values of other cells.

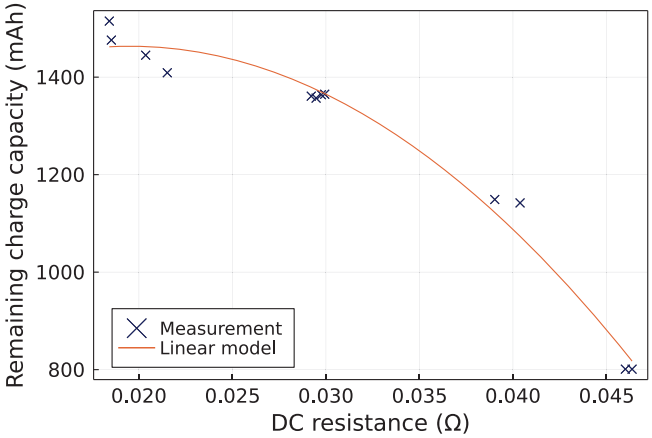

Fig. 7: Relation between the cell internal resistance and SOH.

Fig. 7 shows the measured initial internal resistance values against the remaining charge capacities of the cells at the end of the second-life application. A quadratic-polynomial

curve was also fitted to the data to map the relation between internal resistance and the remaining charge capacities up to 500 cycles, where the ageing kneepoints of cell M7 and M8 are reached. The remaining capacities of the cells are comparable as the cells have the same nominal capacity (2050 mAh). Based on the result, it can be concluded that the higher the initial internal resistance value at the time of the measurement, the faster a cell loses its charge-capacity at the end of the second life. In addition, the quantities follow a quadratic relationship.

V. Conclusion

The internal impedance of a li-ion battery has been shown to provide a key information of the battery SOH. This paper has demonstrated the use of the battery internal impedance measurement in evaluating the battery SOH in a second-life application. Experimental results have shown a clear correlation between the internal impedance and second-life storage capabilities of Li-ion battery cells. The applied method can be used, for example, to rapidly measure a large number of end-of-life batteries and to define their applicability for second-life applications. The future work on the topic will include more experimental studies for different types of battery cells, at different charge/discharge currents and temperatures. Experimental data will also be collected and analyzed to explore different mapping models between battery degradation and the internal impedance.

References

[1] M. E. Market, "Growth, trends, covid-19 impact, and forecasts (2021 - 2026)," Research and Markets (report), Tech. Rep., Apr. 2021.

[2] S. King and N. J. Boxall, "Lithium battery recycling in australia: Defining the status and identifying opportunities for the development of a new industry," *Journal of Cleaner Production*, vol. 215, pp. 1279–1287, 2019.

[3] A. Sonoc, J. Jeswiet, and V. K. Soo, "Opportunities to improve recycling of automotive lithium ion batteries," *Procedia cIRP*, vol. 29, pp. 752–757, 2015.

[4] "Second-life electric vehicle batteries 2020-2030," IDTechEx, Tech. Rep., 2020.

[5] L. C. Casals, B. A. García, and C. Canal, "Second life batteries lifespan: Rest of useful life and environmental analysis," *Journal of environmental management*, vol. 232, pp. 354–363, 2019.

[6] E. Hossain, D. Murtaugh, J. Mody, H. M. R. Faruque, M. S. H. Sunny, and N. Mohammad, "A comprehensive review on second-life batteries: Current state, manufacturing considerations, applications, impacts, barriers & potential solutions, business strategies, and policies," *IEEE Access*, vol. 7, pp. 73 215–73 252, 2019.

[7] X. Wang, X. Wei, H. Dai, and Q. Wu, "State estimation of lithium ion battery based on electrochemical impedance spectroscopy with on-board impedance measurement system," in *Proc. IEEE Vehicle Power and Propulsion Conference*, 2015, pp. 1–5.

[8] D. N. T. How, M. A. Hannan, M. S. Hossain Lipu, and P. J. Ker, "State of charge estimation for lithium-ion batteries using model-based and data-driven methods: A review," *IEEE Access*, vol. 7, pp. 136 116–136 136, 2019.

[9] K. Smith, A. Saxon, M. Keyser, B. Lundstrom, Z. Cao, and A. Roc, "Life prediction model for grid-connected li-ion battery energy storage system," in *Proc. American Control Conference*, 2017, pp. 4062–4068.

[10] M. Broussely, P. Biensan, F. Bonhomme, P. Blanchard, S. Herreyre, K. Nechev, and R. Staniewicz, "Main aging mechanisms in li-ion batteries," *Journal of power sources*, vol. 146, no. 1-2, pp. 90–96, 2005.

[11] E. Martinez-Laserna, E. Sarasketa-Zabala, D.-I. Stroe, M. Swierczynski, A. Warnecke, J.-M. Timmermans, S. Goutam, and P. Rodriguez, "Evaluation of lithium-ion battery second life performance and degradation," in *Proc. IEEE Energy Conversion Congress and Exposition*, 2016, pp. 1–7.

[12] E. Martinez-Laserna, E. Sarasketa-Zabala, I. V. Sarria, D.-I. Stroe, M. Swierczynski, A. Warnecke, J.-M. Timmermans, S. Goutam, N. Omar, and P. Rodriguez, "Technical viability of battery second life: A study from the ageing perspective," *IEEE Transactions on Industry Applications*, vol. 54, no. 3, pp. 2703–2713, 2018.

[13] J. Vetter, P. Novák, M. R. Wagner, C. Veit, K.-C. Möller, J. Besenhard, M. Winter, M. Wohlfahrt-Mehrens, C. Vogler, and A. Hammouche, "Ageing mechanisms in lithium-ion batteries," *Journal of power sources*, vol. 147, no. 1-2, pp. 269–281, 2005.

[14] C. R. Birkl, M. R. Roberts, E. McTurk, P. G. Bruce, and D. A. Howey, "Degradation diagnostics for lithium ion cells," *Journal of Power Sources*, vol. 341, pp. 373–386, 2017.

[15] E. Braco, I. San Martín, A. Berrueta, P. Sanchis, and A. Ursúa, "Experimental assessment of cycling ageing of lithium-ion second-life batteries from electric vehicles," *Journal of Energy Storage*, vol. 32, p. 101695, 2020.

[16] A. Eddahech, O. Briat, N. Bertrand, J.-Y. Delétage, and J.-M. Vinassa, "Behavior and state-of-health monitoring of li-ion batteries using impedance spectroscopy and recurrent neural networks," *International Journal of Electrical Power & Energy Systems*, vol. 42, no. 1, pp. 487–494, 2012.

[17] M. Kassem, J. Bernard, R. Revel, S. Pelissier, F. Duclaud, and C. Delacourt, "Calendar aging of a graphite/lifepo4 cell," *Journal of Power Sources*, vol. 208, pp. 296–305, 2012.

[18] H.-F. Yuan and L.-R. Dung, "Offline state-of-health estimation for high-power lithium-ion batteries using three-point impedance extraction method," *IEEE Transactions on Vehicular Technology*, vol. 66, no. 3, pp. 2019–2032, 2016.

[19] U. Tröltzsch, O. Kanoun, and H.-R. Tränkler, "Characterizing aging effects of lithium ion batteries by impedance spectroscopy," *Electrochimica acta*, vol. 51, no. 8-9, pp. 1664–1672, 2006.

[20] D. I. Stroe, M. Swierczynski, A. I. Stan, V. Knap, R. Teodorescu, and S. J. Andreasen, "Diagnosis of lithium-ion batteries state-of-health based on electrochemical impedance spectroscopy technique," in *Proc. IEEE Energy Conversion Congress and Exposition*, 2014, pp. 4576–4582.

[21] D. D. Macdonald, "Reflections on the history of electrochemical impedance spectroscopy," *Electrochimica Acta*, vol. 51, no. 8-9, pp. 1376–1388, 2006.

[22] E. Samadani, S. Farhad, W. Scott, M. Mastali, L. E. Gimenez, M. Fowler, and R. A. Fraser, "Empirical modeling of lithium-ion batteries based on electrochemical impedance spectroscopy tests," *Electrochimica acta*, vol. 160, pp. 169–177, 2015.

[23] J. Sihvo, D.-I. Stroe, T. Messo, and T. Roinila, "Fast approach for battery impedance identification using pseudo-random sequence signals," *IEEE Transactions on Power Electronics*, vol. 35, no. 3, pp. 2548–2557, 2020.

[24] E. Locorotondo, S. Scavuzzo, L. Pugi, A. Ferraris, L. Berzi, A. Airale, M. Pierini, and M. Carello, "Electrochemical impedance spectroscopy of li-ion battery on-board the electric vehicles based on fast nonparametric identification method," in *Proc. IEEE International Conference on Environment and Electrical Engineering and IEEE Industrial and Commercial Power Systems Europe*, 2019, pp. 1–6.

[25] J. Sihvo, T. Roinila, and D.-I. Stroe, "Broadband impedance measurement of lithium-ion battery in the presence of nonlinear distortions," *Energies*, vol. 13, no. 10, 2020.

[26] A. Fairweather, M. Foster, and D. Stone, "Battery parameter identification with pseudo random binary sequence excitation (prbs)," *Journal of Power Sources*, vol. 196, no. 22, pp. 9398–9406, 2011.

[27] K. Godfrey, "Introduction to binary signals used in system identification," in *Proc. International Conference on Control*, 1991, pp. 161–166.